Investigation of Coal Particle Gasification Processes with Application Leading to Underground Coal Gasification

Tata Sutardi [a, b], Manosh C. Paul [a,*], and Nader Karimi [a]

[a]Systems, Power & Energy Research Division, School of Engineering, University of Glasgow, Glasgow G12 8QQ, UK

[b]Agency for the Assessment and Application of Technology (BPPT) – Republic of Indonesia

*Corresponding author: Tel: +44 (0)141 330 8466, E-mail: Manosh.Paul@glasgow.ac.uk

Abstract

A coal particle model is developed to investigate the thermochemical processes of gasification for underground coal applications. The chemical reactions are defined with an Eddy Break up (EBU) model for controlling the reaction mechanisms and the study is particularly focused on identification of the important kinetic parameters, which control the consumption rate of coal mass. As an initial validation, the coal particle oxidation based on the experimental results is used for comparison. The gasification reactions are subsequently applied for the thermochemical process investigation, and the results show that the best agreement of coal oxidation is achieved by the pre-exponent factor *(A)* of 0.002 and 85500, for the reactions, R2 ($C + O_2 = CO_2$) and R3 ($C + 0.5O_2 = CO$), respectively. The kinetic parameters for the gasification process of coal particle leading to the syngas production are also optimised. The results show that the production of H_2 and CO is controlled significantly by the level of oxygen concentration in the char reactions. However, their chemical rates are strongly dependent upon the reaction zones. For example, CO is produced in both oxidation and reduction reaction zones, while H_2 production is dominated in the reduction zone. Spatio-temporal distributions of the gas species along with the coal particle temperature provide additional information for further development of UCG modelling. Ultimately, the model gives a good guideline with the associated thermochemical processes that can help developing advanced coal gasification technology and lead to improved syngas quality.

Keywords: Thermochemical process, kinetic reaction, Computational Fluid Dynamics, coal particle gasification, Underground Coal Gasification

Nomenclature

Roman Symbol

h_s	Heat source (W/m^2 K)
A	Pre- exponential factor (unit vary)
A_p	Surface area of particle (m^2)
C_g	Reactant gas concentration (kmol/kg)
D_m	Diffusion coefficient (m^2/s)
E_a	Activation Energy (J/kmol)
F	External force (N)
g_i	Gravitational acceleration
M_i	Molecular weight of species *i*
M_w	Molecular weight of solid reactant
R_c	Universal gas constant, (J/K.mol)
Y_i	Mass fraction of species *i*
k_i	Reaction rate coefficient for reaction *i*
k_m	Mass transfer coefficient
m_i	Mass fraction
p_{ij}	Rate exponent of reacting species
h	Enthalpy (kJ/kg)
J_i	The flux of species *i*
S_m	Source of mass (kg)
Sh	Sherwood number
T	Temperature (K)
YY	Mass stoichiometric coefficient
M	Mass of particle (kg)
p	Pressure (Pa)
R	Rate of consumption of solid reactant (kg/s)
r	Radius
$C_{\varepsilon 1};\ C_{\varepsilon 2}$	Model constant
t	Time (s)
x	Distance/displacement (m)
u	Velocity (m/s)
t_{id}	Ignition delay time
t_{cv}	Coal volatile burnt out time
t_{char}	Char burn out time
T_{cv}	Maximum temperature coal volatile combustion (K)
T_{char}	Maximum temperature char combustion (K)

Greek Symbol

α_i	Particle volume fraction
β	Temperature exponent
τ_{xr}	Stress tensor
$\emptyset$	Ratio of stoichiometric of solid and gas reactant
ρ	Density (kg/m^3)
ρg_x	Gravitational body force
μ, λ	Viscosity coefficient (kg/m.s)
σ	Turbulent Prandtl number
δ	Kronecker delta

Subscript

p	Particle
x, r, i, j	Direction and species or phase
cv	Coal volatile matter
k	Turbulent kinetic energy (m^2/s^2)
ε	Turbulent dissipation rate (m^2/s^3)

1. Introduction

The Survey of Energy Resources was carried out in 2013, and estimated that the world coal reserves are approximately 890 billion tonnes [1]. The trend of world coal consumption also increases from 2012 to 2040 at an average rate of 0.6% per year, from 6885 million tonnes in 2012 to 8100 million tonnes in 2040. The top three coal-consuming countries are China, the United States of America, and India, which together account for more than 70% of world coal use [2]. It is predicted that there are greater resources deep underground that could increase the proven coal reserves, but these are not mineable with current technology. Underground coal gasification (UCG) is an option to utilize this type of coal reserve [3, 4]. UCG allows the use of coal seams which are technically difficult to exploit (too thin, too deep, steeply dipping, seams of low ranked coals, etc.).

UCG is defined as a thermochemical process to produce gaseous fuel (syngas) as well as a wide range of chemical syntheses directly from the coal seam. The main chemical processes occurring in coal gasification are drying, pyrolysis, combustion, and gasification of solid hydrocarbon. The final product gas composition and heating value depend on the thermodynamic conditions of the operation (e.g. temperature and pressure), coal composition itself, as well as the gasification agent [5].

Based on the reaction area in a gasification channel, there are three zones – oxidization zone (the major products are carbon dioxide and carbon monoxide [5]), reduction zone, and dry distillation zone [6]. In the oxidization zone, multi-phase chemical reactions between oxygen contained in the gasification agent and carbon in the coal seam surface occur, increasing the coal temperature and producing heat. The coal seams become incandescent or flaming at this stage, with a temperature variation around 1200 K to 1600 K [7]. Inherent moisture plays a role in coal oxidation, affecting oxygen transport in coal pores and participating in the chemical reactions during the oxidation [8]. By the time the O_2 is gradually consumed, the gas stream comes into the reduction zone. In the reduction zone, H_2O (steam) and CO_2 are reduced to H_2 and CO with a high temperature effect, when they meet with the incandescent coal seams. The temperature ranges from 900 K to 1300 K, and the length is 1.5 - 2 times that of the oxidation zone with its pressure being 0.01 - 0.2 MPa [9].

The overall UCG process is strongly exothermic, and temperatures in the burning zone are likely to exceed 1200 K. After conductive heat loss to the surrounding strata and convective heat loss to native groundwater, syngas typically flows through production wells at temperatures between 500 K and 700 K. Around the burn zone, the high buoyancy of hot syngas to the groundwater tends to lead to large pores being invaded by bubbles of syngas, which could heat the groundwater and change it into steam. A dynamic interface between steam and hot groundwater will develop around the UCG burn zone, and, in that, steam could mix with the syngas [10]. This effect could be one of the important reasons for controlling the temperature and chemical reactions in the gasification process for UCG application.

Although a number of UCG field trials have been performed, the information on the detailed UCG process for modelling application is still limited. It is because of the high cost on extracting data as well as the difficulty in controlling/monitoring the operating variables. As a result, and due to this limitation, several laboratory-scale experiments have been reported [11-15] and also some numerical models have been developed [16-22]. Prior to 1975, the development of UCG models was very limited. Over the years, several approaches have been developed for the modelling of the UCG process, such as packed bed model, channel model, and coal slab model [20]. Most of the earlier models were one-dimensional (1D) [16]; however, with the advancement of computational power, two-dimensional (2D) or even a few three-dimensional (3D) models were developed [23-26]. Nevertheless, an important aspect of UCG modelling which relates to the identification of thermochemical behaviour of coal gasification reactions for syngas production as well as cavity formation needs to be developed further. Coal consists of multiphase chemical species such as volatile matter, char, moisture and ash, and the species reactions result in the syngas production and subsequently, cause a shrinkage of coal mass. In a UCG operation, this coal mass shrinkage causes the cavity formation. Previous modelling studies reported the syngas production and cavity formation of UCG [22, 25] by considering coal as a porous medium [25] with a fast chemistry and surface reaction mechanism for gasification. Compared to these existing investigations, the work presented in this paper takes a totally different approach in which coal is presented as a multiphase component of solid and fluid, where the reaction processes of UCG are investigated through a coal particle based gasification process modelling, as shown in Figure 1. The method proposed will be more reliable when presenting the coal properties and multiphase reactions and also for controlling the gasification

reaction mechanisms. Moreover, investigating the cavity formation as an effect of the chemical reaction mechanisms, and possibility of identifying the coal mass shrinkage and how it affects further on the cavity formation would provide a great advantage. Further, this model offers a solution on the flame and temperature propagation through the particle by simultaneously decreasing the particle mass itself along the reactions. To the best of our knowledge, none of the previously published papers on numerical modelling considered these mechanisms simultaneously.

Figure 1 presents the gasification processes of UCG and how each of these is directly linked to the gasification of a coal particle, which is considered to be a micro scale coal block in deep underground. As clearly identified in this figure, the reaction mechanisms of coal gasification, irrespective to the scaling of the model are essentially the same, and mainly consist of the processes of devolatilization / pyrolysis, oxidation, and reduction [27]. Therefore, the proposed particle based computational model provides the opportunity to investigate the fundamental aspects of the thermochemical physics usually occur in UCG. It also provides an additional flexibility to identify the effects of various relevant operating and boundary conditions on gasification. A full scale UCG simulation model, on the other hand, may be developed. However, without any doubt, it would be highly cumbersome and computationally expensive to run each model case based on the parametric optimisations as being planned. Moreover, the particle based modelling approach allows for the prediction of the coal mass shrinkage during the reactions, which remains very difficult with the surface reaction model [22, 25, 26]. In UCG process, the contact area between the coal seam surface and hot gas changes over time, resulting in a dynamic boundary condition at the interface. The propagation of combustion front also causes the coal mass loss and results in gas products. Therefore, the coal mass loss causes the boundary layer propagation or displacement of the contact area. The particle model will address this challenging issue of defining a dynamic boundary condition to be encountered in the computational modelling of UCG.

Initially, the study is focused on the investigation of the thermochemical reaction processes using the UCG reaction mechanisms sourced from Ref [25]. Then, the processes will be kinetically controlled and their effect on the gasification will be investigated, with an aim to predict the best possible gasification conditions that would lead to quality gas products. Various operating parameters including the fuel composition, kinetics properties, and gasification agents

are also the subjects of investigation in this work. The model is validated at the initial stage with suitable experimental data collected from literature. The key objectives of this current study are,

- to investigate the thermochemical behaviour of coal gasification with a particular focus on the suitability of the chemical reactions available in the literature in predicting the process of coal gasification;
- to study the mechanism and identify the parameters for controlling the gas production through gasification;
- to predict and monitor the gas products and coal particle temperatures behaviour;
- to initiate the new model approach on modelling of UCG's boundary condition, which consider coal mass reaction

2. Gasification Reaction Mechanisms

The initial process during coal gasification is drying, which liquid water leaves coal particle in the form of steam. Afterward devolatilization/pyrolysis which is related to gas or volatile matter released from coal or the heating/reaction process in the absence of oxygen. Combustion is the coal reaction with oxygen to produce CO_2 and H_2O. Gasification then follows and leads to the production of syngas [28].

As seen in Table 1, the reaction mechanisms in UCG consist of thirteen chemical reactions [25]. The reactions R1, R2, R3, R4, R5 and R6* take place on the wall plane of coal seams between the gas and solid coal (heterogeneous reactions), while the other reactions occur between one gas and another (homogeneous reactions). These reactions are considered as devolatilization reactions for the initial stage, then continued by the homogenous and heterogeneous reactions that occur simultaneously. A kinetic method is used for controlling the mechanism of chemical reaction rate. This method will be able to give information about the reaction mechanisms, intermediate chemical reaction states, and the process of how different conditions influence the rate of chemical reactions [29].

Through devolatilization or pyrolysis, raw coal is converted to volatile matter and char as an effect of external heat in the absence of the oxygen [24]. The devolatilization reaction is written as

$$Raw\ coal\ (s) \xrightarrow{k_1} (YY)\ Coal\ volatile\ (g) + (1 - YY)C(s) \qquad \text{R1}$$

Here *s* and *g* denote solid and gas respectively. The mass continuity for the raw component in coal particle *p* is describe as

$$\frac{dm_p}{dt} = -R_p, \tag{1}$$

where the net rate for raw coal consumption is given by

$$R_p = k_1 \alpha_p m_p, \tag{2}$$

and the rate of production for coal volatile is described as

$$R_{cv} = k_1 YY \alpha_p m_p, \tag{3}$$

where the reaction rate coefficient is the Arrhenius form given by

$$k_1 = AT^{\beta} exp\left(\frac{-E_a}{R_c T}\right). \tag{4}$$

Particle and gas reactions begin once the volatile fraction of raw coal particle has completely evolved. The heterogeneous reaction is a process where a solid component reacts with a gas-phase component to form other species products. In this simulation, the initial reaction for the heterogeneous reaction is the oxidation of coal particle (char) to become carbon dioxide [30] (R2 in Table 1), followed by the four other heterogeneous reactions (R3 - R6*). In the simulation, the heterogeneous reaction rate is determined by the combined effect of the Arrhenius rate and gas-reactant diffusion rate to the particle surface. The model of particle rate consumption is determined by [31, 32]

$$R = \frac{dm_i}{dt} = -\frac{k_m k}{k + k_m} \emptyset C_g M_w A_p, \tag{5}$$

where,

$$k_m = \frac{Sh\, D_m}{d}. \tag{6}$$

Finally, the homogeneous reactions (R7 - R13*) occur between the gas species in the gasification reaction, as defined in Table 1. The reaction rate of each of the homogeneous reactions as a function of the composition and the rate constant is determined by the following equation

$$R_j = R_{i,kin} = -k_j \prod_{all\ reactants} \left(\frac{\rho Y_i}{M_i}\right)^{p_{ij}}. \tag{7}$$

3. Coal Particle Model Development

The simulation is initially developed based on the experimental study of coal combustion in [33], which is extended further by considering the modelling of coal particle gasification. Drop tube furnace (DTF) facilities were used in this experiment [33], with a coal particle injected into the furnace from the top. The simulation uses a single coal particle injection model to validate results with experimental data, then the injection pattern is changed to a steady model for further investigation. Raw coal transformation and gas component production are investigated through the simulation, and results are assessed for further application.

3.1 Governing equations

The governing equations that are used in this simulation are the continuity, momentum, chemical of species, conservation of energy, and transport equations. The continuity equation is written as [34]:

$$\frac{\partial \rho}{\partial t} + \frac{\partial (\rho u_x)}{\partial x} + \frac{\partial (\rho u_r)}{\partial r} + \frac{\rho u_r}{r} = 0, \tag{8}$$

the equation for the axial of momentum conservation:

$$\begin{aligned} &\frac{\partial (\rho u_x)}{\partial t} + \frac{1}{r}\frac{\partial (r\rho u_x u_x)}{\partial x} + \frac{1}{r}\frac{\partial (r\rho u_r u_x)}{\partial r} \\ &\quad = -\frac{\partial p}{\partial x} + \frac{1}{r}\frac{\partial}{\partial x}\left[r\mu\left(2\frac{\partial u_x}{\partial x} - \frac{2}{3}(\nabla \cdot \vec{u})\right)\right] \\ &\quad + \frac{1}{r}\frac{\partial}{\partial r}\left[r\mu\left(\frac{\partial u_x}{\partial r} - \frac{\partial u_r}{\partial x}\right)\right] + \rho g_x \end{aligned} \tag{9}$$

the equation for the radial of momentum conservation:

$$\begin{aligned} &\frac{\partial (\rho u_r)}{\partial t} + \frac{1}{r}\frac{\partial (r\rho u_x u_r)}{\partial x} + \frac{1}{r}\frac{\partial (r\rho u_r u_r)}{\partial r} \\ &\quad = -\frac{\partial p}{\partial r} + \frac{1}{r}\frac{\partial}{\partial x}\left[r\mu\left(\frac{\partial u_r}{\partial x} - \frac{\partial u_x}{\partial r}\right)\right] \\ &\quad + \frac{1}{r}\frac{\partial}{\partial r}\left[r\mu\left(2\frac{\partial u_r}{\partial r} - \frac{2}{3}(\nabla \cdot \vec{u})\right)\right] - 2\mu\frac{u_r}{r^2} + \frac{2}{3}\frac{\mu}{r}(\nabla \cdot \vec{u}) \end{aligned} \tag{10}$$

where, $\nabla \cdot \vec{u} = \frac{\partial u_x}{\partial x} + \frac{\partial u_r}{\partial r} + \frac{u_r}{r}$, and ρg_x is the gravitational body force.

The concentration of species can be expressed in terms of the mass fraction, $m_i(x, r, t)$, or the concentration of species $C_i = m_i \rho$, which is defined as the mass of species per unit volume. The conservation law of chemical species is represented as,

$$\frac{\partial}{\partial t}(\rho m_i) + \nabla \cdot (\rho m_i V + J_i) = R_i, \tag{11}$$

where, R_i is the account for the production or consumption of the species by chemical reaction.

The energy equation in this simulation may be written as [34]:

$$\frac{\partial(\rho E)}{\partial t} + \nabla.(u(\rho E + p)) = -\nabla.\left(\sum_j h_j J_j\right) + h_s \tag{12}$$

In this equation, E is the total energy, and h_s as heat generation includes heat of chemical reaction, any inter-phase exchange of heat, and any other user-defined volumetric heat sources. In the simulation, the equation state of gas in the reaction is treated as ideal gas. Thus, this equation is needed to connect with the thermodynamic variables such as, $p, \rho,$ and T.

For accommodating turbulent flow, Reynolds-averaged Navier-Stokes (RANS) form of the above equations is solved with a realizable $k - \varepsilon$ model [35].

The equation of motion for the particle is defined as,

$$m_p \frac{d\overline{u^p_{i,J,k}}}{dt} = \sum \bar{F}. \tag{13}$$

Since the particle size used in this simulation is small, the lift force of the particle is neglected. But, the effects of the drag and gravity forces are included since they have influence on the parameters of investigation.

3.2 Geometry of model and boundary conditions

The geometric model, as illustrated in Figure 2 (a), is considered to be a cylindrical furnace (Drop Tube Furnace (DTF) shape) with an internal diameter of 7 cm. The heated wall section of the furnace was 25 cm measured from the inlet, and coal particle injection starts from the centre of

the inlet. An axi-symmetric model was used for the simulation, and in Figure 2(b), a grid distribution with the boundary conditions used is shown.

From the experimental data [33], the initial boundary condition for the simulation is defined, as can be seen in Figure 2. The furnace was initially heated up with hot air at 1200 K before the coal being injected, while the furnace wall temperature was maintained at 1400 K. The inlet air velocity was 0.045 m/s. The simulation is run to establish a fully-developed flow and in order to accommodate the development region, the furnace wall was extended to 75 cm and this portion kept adiabatic.

3.3 Coal properties and grid selection

Simulation of coal particles is carried out for a bituminous coal sample of PSOC 1451; for detailed properties, such as its proximate and ultimate analyses, see Table 2 [33].

The table gives important information that is used to define the chemical compounds of coal and its volatile contents. Since the focus is only on the gasification process, sulphur (S) elements from the ultimate Dry-Ash Free (DAF) analysis are neglected. Further, based upon the proximate and ultimate correlations, the coal volatile composition is defined as $CH_{2.7}O_{0.248}N_{0.058}$ with the *YY* value of 0.29, as stated in the reaction balance equation R1. Kinetic properties of the coal needed for the simulation are sourced from the literature and presented in Table 3.

The coal particle simulation is conducted under a quiescent gas condition in the furnace and it is set by turning off the hot air flows a few seconds prior to the particle injection. This treatment supports the creation of a homogeneous furnace gas temperature at around 1400 K. The coal particle diameter used is $75\mu m$, which is the size commonly used in pulverized coal power plants, and modelled as a spherical particle.

In order to estimate the grid size and mesh quality required for the simulation, a grid-refinement test is carried out using 4 types of grid size with a total cell number of 20,944; 23,760; 29,925; and 35,916 respectively. This simulation has been done prior to the coal particle injection, and the gas temperature used as a parameter of comparison. The effects of the grid size variation are presented by the gas temperature variation of each grid size along the axis (x – direction) and along the radial directions, as they can be seen in Figure 3,

Figure 3 shows that all the cell numbers obtain the almost similar temperature profile along the axial and radial directions, which indicate that any of these will be suitable for the simulation. The maximum and minimum temperatures obtained are similar, but the three higher number of grid cells give the best agreement when comparing the maximum temperature. The same behaviour is obtained for the radial direction at several distances along the axis, as shown in Figure 3(b), (c), (d), and (e). However, to avoid any potential issue with numerical stability and also considering the computational time, the grid size of 29,925 cells is used to perform all the numerical simulations.

3.4 Overview of the Numerical Procedures

STAR-CCM CFD software is used for developing the coal particle gasification model. Gas chemical species reactions are defined and an Eddy Break up (EBU) model with the kinetic control parameter is implemented for controlling the reaction mechanisms. EBU model is used for modelling of reacting flow with fast chemistry, and reaction rate is determined by the rate at which turbulence can mix the reactants and heat. The kinetic properties of each reaction have an important role in controlling these reaction mechanisms. Coal particles interaction with the fluid region is dealt with through the Lagrangian multiphase model. Coal particle properties are defined and an injector is set up for controlling the particle injection into the furnace. The interaction of these species and heat/energy in the fluid region are governed through the transport equations already described in the previous section.

The model of numerical simulation is developed based on the experimental condition, and then this result is validated. In the numerical simulation, coal particle behaviour inside the DTF is represented as a single coal particle injected into the furnace. Some parameters such as combustion time, species component fraction, and temperature profile can be identified through the simulation and then compared to the experimental result. As mentioned in the previous section, the kinetic parameter have important role in controlling the reaction mechanisms. Table 3 provides the reference values of kinetic properties that can be considered for each reaction [24].

R1 to R5 and R7 to R8 are reactions for coal particle oxidation/combustion, and R6* and R9* to R13* are additional reactions applied for coal particle gasification. The validation is applied for coal oxidation stage, with the aim of finding the suitable set of kinetics properties for this model simulation.

4. Process Investigation with Validation

The model validation is an important stage of the current work. For this purpose, the experimental result of coal particle combustion [33, 36, 37] is used as a reference for validation of coal particle oxidation. At this stage, only the reactions of coal combustion/oxidation have been used, and they are controlled by a set of kinetic parameters value. There are several numbers of kinetic values used in the literature cited, but for an initial simulation the set of kinetic values of *Blaid et al.* is used [38]. For identification, it is called Simulation 1. The comparison result of Simulation 1 and the experimental result can be seen in Figure 4.

The green line in this figure represents the coal particle combustion behaviour based on the experimental testing. This result show that the bituminous coal (PSOC-1451) consistently exhibited two peaks in each profile, an exceedingly strong first peak followed by a significantly less pronounced second peak as seen in the green line [33]. The first peak is attributed to volatile matter burning homogenously with air, which typically lasted for ~20 ms (milliseconds) after ignition delay time (t_{id}) and it is identified as burning out time for volatile matter (t_{cv}). The second peak is attributed to heterogeneous combustion of char residue lasted for ~140 ms (t_{char}). Simulation 1 shows that the temperature and char mass fraction profiles, as seen as the blue dash-dot and red dashed lines, respectively. The blue line shows that the coal particle increases temperature rapidly to ~2200 K (T_{cv}) within ~20 ms after coal injected, that indicates a good agreement for the ignition delay time and also the maximum temperature of coal volatile combustion (T_{cv}) with the experimental result. After this point, the particle temperature of the experimental result drops and increases again from ~40 ms, but this was not shown in temperature of Simulation 1. Instead, the particle temperature of Simulation 1 (the blue line) shows a sharp drop to its minimum at ~80ms and then finally reaches ~1400K. This temperature drop further indicates an absence of char combustion, as also evidenced by the result of the char fraction (the red line), which remains stable at a value of around 0.85. Clearly, the char reactions did not occur, and this is considered to be a limitation of the set kinetic values utilised in the four reactions of char combustion (R2 to R5), Table 1. R2 and R3 represent the exothermic reactions and the others are endothermic. Simulation 1 failed to model the coal particle burning that would lead to the production of heat and subsequently, increase the particle temperature. So, it is essential to focus first the investigation on the exothermic reactions which potentially might have caused this issue, followed by the investigation on the other relevant reactions. This part of

the investigation is summarised in the sections below considering variation in the properties of the chemical kinetics reactions.

4.1 Investigation of the kinetic parameters of R2 and R3

The reaction kinetic rate (k) is affected by the set of kinetic parameters used in the Arrhenius equation (4). The effects of the kinetic parameter values of R2 and R3 as a function of temperature can potentially cause a different reaction rate for char [39]. As mentioned previously, the initial Simulation 1 used the set of kinetic values based on the study of *Blaid et al.*[38]. Both of R2 and R3 in this case have the lowest reaction rates compared to the other results, and it is thus understood that these rates are slow compared to the other reactions and hence, the char remained unaffected. Kinetic values of R2 and R3 from the several other references are sourced and subsequently, applied to the simulation model to examine the char reaction rates. Using the kinetic parameter values of R2 and R3 presented in Table 3, a combination of 15 different simulation models is generated and their simulation IDs can be seen in Table 4.

4.2 Validation process of coal oxidation

For the validation purpose, the parameters to be compared between the experimental and simulation results are

- the maximum temperature of coal volatile combustion (T_{cv}),
- the maximum temperature of char combustion (T_{char}),
- the ignition delay time (t_{id}),
- the coal volatile matter burning out time (t_{cv}), and
- the char burning out time (t_{char}).

The set of kinetics properties that produce the best agreement between them will be considered and used further on the coal gasification investigation.

The maximum temperature of coal volatile matter combustion (T_{cv}) and char combustion (T_{char}) is compared in Figure 5. As seen in Figure 5(a), the experimental T_{cv} is ~2250K [33, 37] with a 5% deviation reported in these studies. The comparative plot shows that almost all of them are within the acceptance range, except for Simulations 7, 11, and 15. However, considering the maximum temperature of char combustion (~1860K [33]) presented in Figure 5(b), it clearly

indicates that the set of kinetic parameters used in Simulation 3 produce the results that give the best agreement of T_{char} with the experimental result.

Similar conclusion can also be drawn from the comparisons of the results of the ignition delay time (t_{id}), coal volatile combustion time (t_{cv}) and char burning out time (t_{char}) illustrated in Figure 6. According to the literatures [33, 37], the ignition delay time is ~10 to 20 ms, and the coal volatile combustion time lasts for another ~10 to 20 ms. Although the simulation results of t_{id} in Figure 6(a) show that all the kinetic parameters provide results with very good accuracy, the char burning out time (t_{char}) is clearly predicted to be different in Figure 6(b). Note that the char burnt out time is determined by calculating the interval of time taken to completely burn the char i.e. the time between the maximum and minimum/zero fractions of char. The experimental result suggests that the burnt out time for char (t_{char}) is ~140 ms while the burning out time of coal particle is ~180 ms [33]. As seen in Figure 6(b), only Simulation 3 achieved the burning out time of coal particle within ~180 ms and also burning out time of char ~140 ms. Other simulations predict the burning out time of char to be more than 500 ms, or much shorter than the experimental value. Therefore, this validation exercise further confirms that the set of kinetic parameters of R2 and R3 used in Simulation 3 for the coal particle oxidation is the best suited for this model. Thus, this set of values to be considered for further development and investigation of gasification.

Nevertheless, before these set of kinetic parameter values are applied to a gasification case, it is necessary to re-consider other reactions as well and investigate their potential effects on the coal oxidation.

4.3 The effect of other combustion reactions

As described in the previous section, the validation procedures only considered the exothermic process of char reactions. In this section, the various kinetic parameter values of other reactions for the coal oxidation will be investigated. Simulation 3 is taken as a reference case, and then the other set of kinetic parameters values for R4, R5, and R8 are examined taking into account the various available data sourced from the literature as shown in Table 5 with their individual Simulation ID. The investigation in this section is limited to the char burnt out time (t_{char}) and the maximum char temperature (T_{char}), since the main focused is on the char reaction.

Figure 7(a) and (b) show the results of variation of the kinetic parameters of R4, and as shown, the same behaviour is obtained for both the char burnt out time and the particle temperature

profile from each. It therefore indicates that these variations do not have any effect on the char decomposition process. Figure 7 (c)-(d) and (e)-(f) also show the same having the results unaffected by the variation of the kinetic parameters of R5 and R8. They all have agreement with the results of Simulation 3, or in other words, confirm that all the kinetic parameter values for R4 (i.e. Simulation 3 case) can be considered for further development of coal particle gasification.

However, it should be further noted that representing the proper kinetic properties for the char oxidation is crucially important for this research, because it initiates the gasification process as illustrated in Figure 1. Oxidation is an initial process of coal gasification, and it is followed or simultaneously occurs with other process such as pyrolysis and reduction for completing the gasification process. The coal combustion (oxidation) process has now been validated, and the set of kinetic parameter values based on Simulation 3 are chosen for the oxidation process. For the development of coal particle gasification investigation, relevant reactions describing the gasification mechanisms, as in Table 1 and Table 3, are included in the numerical model.

5. Investigation of Gasification Performances

The coal particle gasification reactions are developed by inclusion of the pyrolysis and reduction reactions into the coal combustion mechanisms as seen in Table 1. Similar to the combustion model, some reactions have more than one kinetic parameter values as in Table 3, and therefore, an investigation on this is needed to find out the suitable value for the gasification application.

5.1 Identification of kinetic parameter for gasification reactions

The reactions of gasification with more than one kinetic parameter values are R9*, R10*, R11*, and R12*. To investigate the effect of the variation in the kinetic properties, Simulation 3 is used as a base case. A combination of simulation models generated with their simulation IDs can be seen in Table 6. Ten simulations were conducted, and the comparisons between the results of CO, H_2, CO_2 and CH_4 as the products derived from these simulations are presented in Figure 8.

Figure 8(a) and (b) represent the kinetic value variations of R9* on the gas products H_2 and CO, and CO_2 and CH_4, respectively. The simulations result in almost similar fraction of the gas products for each variation implemented and thus, affirm that all the variations in the kinetic parameters for this reaction have a negligible effect on the gas productions. The same behaviour is seen for the other reactions R10*, R11* and R12*, as shown in Figure 7(c) and (d); Figure 7(e)

and (f); and Figure 7(g) and (h), respectively. Hence, all the set of the kinetic parameters can be considered for the coal gasification development. However, this paper considers the kinetic parameter identified by "A" letter IDs.

5.2 Coal particle gasification

The value of set kinetic parameters for each reaction has been decided, and will be implemented for gasification process. The single coal particle gasification is applied as an initial model application. This application will be compared with the combustion model to give better understanding about the process difference. The results can be seen in Figure 9.

Figure 9(a) shows a comparison between the behaviours of char and volatile matter reactions, which indicates both process are similar. However, Figure 9(b) shows the results of CO_2 and H_2O though trend to be similar, only on the gasification process produces CH_4. Figure 9(c) shows the H_2 and CO production of the coal particle combustion and gasification, and the difference in the results clearly identified by the two different processes utilised. In particular, H_2 from the gasification process is much higher than that from the combustion process. Yet, this is not the case when comparing the CO production. Usually, CO production is expected to be higher and CO_2 lower in the gasification process, but the process is controlled by an excess amount of oxygen inside the reactor.

Figure 9(a) and (c) further indicate a correlation between the char and the production of CO and H_2. They show that the CO and H_2 productions occur when the coal particle/char exists in the reactor, and they decay after the coal particle/char burnt out. This behaviour needs to be clarified further in order to attain better understanding on the CO and H_2 production and the investigation is presented in the section below.

5.3 Controlling char and oxygen concentration

Maintaining char as well as controlling the oxygen concentration in the reactor had indicated having an effect on the gasification process as already shown in Figure 9. Further simulation is performed to clarify the gasification behaviour firstly, by injecting coal particle continuously into the reactor to maintain the char inside the reactor, and secondly by simulating the continuous injection gasification process in various oxygen concentrations inside the reactor to identify their effects on the formation of CO, H_2 and CO_2. For these purposes, coal particle is injected every 50 ms and last for 20 s. The result of these simulations can be seen in Figure 10.

Figure 10(a) shows that maintaining char inside the reactor causes continuous production of H_2 and CO. This result thus further confirms how important the char reaction on the gasification process is.

Figure 10(b), (c) and (d) show that the effect of oxygen concentration inside the reactor on the syngas products, CO, H_2 and CO_2, respectively. Figure 10(b) shows the maximum concentration of CO at 5% and 2% oxygen are higher than that in the air condition. Figure 10(c) shows how the oxygen concentration affects the H_2 production. The H_2 production initially slows down because of the reduction in the oxygen supply, but crosses over the concentration shown at an air condition. Finally, Figure 10(d) shows how the CO_2 production in the reactor is affected. Initially, the conditions at 5% and 2% oxygen produce lower CO_2 than at air condition, but after ~10 s their concentrations cross over and become higher than the air condition. This result indicates that the excess oxygen still occurred in the reactor, and it potentially supported the CO_2 formation.

5.4 Reaction process of coal particle gasification analogous to UCG application

Controlling the oxygen concentration in the gasification process, as illustrated in the previous section, is very important, since it affects significantly the reaction kinetics. In the case of a UCG process, through the oxidation process coal gradually burns up and the resulting products flow towards the downstream where the reduction processes occurs and finally, the product gases are collected through a bore hole. In the simulation, continuously injected coal particles flow through the channel under a quiescent gas condition [40], and the oxidation reaction propagates through the downstream due to the presence of air. The reduction process reactions occur simultaneously at the back the oxidation, thus compared to a UCG, the process described may also be considered occurring in the reverse direction.

In this model, the continuous injection flowrate of the coal particle is increased to 500 times which results in the increased production of char, and the simulation results are presented in Figure 11.

Figure 11 shows the contour plots inside the reactor of gases O_2, CO_2, CO and H_2 at different times up to the period of 115 s. Figure 11(a) shows initially the oxygen concentration dominants in the reactor and from the time when the coal particle is injected, the oxygen concentration at the upstream decreases and finally disappears. This behaviour represents the oxidation process

of the coal particle. Opposite effect is shown on the CO_2 production, as shown in Figure 11(b). The CO_2 concentration initially at its minimum (zero), but over the time of the oxidation reactions, its magnitude increases and finally becomes dominant in the reactor as seen at ~105 s after the coal particle injected. Correlating the CO_2 decrease at this area with the CO formation, Figure 11(c) indicates the CO formation at the same position. It is possible that CO_2 reacts with solid carbon to form CO through the reduction process. Finally, Figure 11(d) shows the H_2 production in the reactor. Initially, the H_2 production occurs in the oxidation zone, but over the time it can be seen that its production is greater in the reduction zone. It thus further indicates that this gas is potentially produced more in the reduction zone (less of oxygen area).

The gas production behaviour as explained earlier, describes the thermochemical process of chemical reaction mechanisms of coal gasification. Generally, this behaviour has an agreement with the UCG mechanism as described in reference [29]. However, it is occurred in the reverse direction to the UCG gas flow, since the model uses the flowing coal and quiescent gas/air inside the reactor. Nevertheless, all the oxidation and reduction reactions identified occurred, as evidence by the gas production seen clearly in each of the reaction zones.

6. Conclusion

The simulation model of coal particle gasification has been considered in this paper for simplifying the understanding of complex thermochemical reaction mechanisms of coal gasification. This understanding is important for obtaining of the better syngas production and will be used further for developing a robust method of UCG modelling.

The UCG reaction mechanisms based on the references are used to present the thermochemical behaviour of UCG through the simulation model. This paper has started using coal particle gasification model as an initial development for more complex model such as particle bed packed model study.

The key results related to gasification mechanism that could be taken from this simulation are as follows:

- The kinetic parameter properties have an important role in developing coal particle gasification simulations, and their value is specific especially on the oxidation mechanisms. By simulating these parameters based on the references sources, the

proper set of kinetic parameters values have been validated and considered for the gasification model presented.

- The coal particle model can be applied to support the investigation of thermochemical process of gasification. As a result, the behaviour of char reaction, gas reaction, and syngas production in the gasification process can be seen. The single coal particle simulation results show that the syngas production stops after the char burns out, and it indicates the important role of char in the gasification process.
- The simulation results show the importance of controlling the oxygen concentration and char in order to obtain the better gas productions. The increasing of CO_2 indicates more O_2 supply in the gasification process; therefore, in the single coal particle case of simulation the oxidation process occurs along the reaction, and the fuel equivalence ratio used in this simulation is very small (~0.0000041).
- The thermochemical process of coal gasification process can be described through the coal particle model simulation. The oxidation and reduction process that occurred in the UCG process can be illustrated and understandable through this simulation.
- For future work consideration, the study on the effect of environment to the gasification process considered to be applied. In order to improve this approach into further application of UCG, this particle simulation would be considered as a bed packed model.

Finally, these simulation results indicate a good guideline for obtaining better quality syngas production, and initiate the new model approach on controlling the coal seam reaction mechanisms as a part of UCG modelling development.

7. Acknowledgements

The first author gratefully acknowledges the Ministry of Research, Technology, and Higher Education (KEMENRISTEKDIKTI) of Republic Indonesia for the scholarship funding through the Research and Innovation in Science and Technology Project (RISET-Pro) program and also the University of Glasgow for supporting this research.

References

[1] W. E. Council, 2013 "*World Energy Resource - 2013 Survey*," in *Report - Survey, ISBN : 978 0 946121298*, ed, p. 1.2.

[2] DOE/EIA, (2016)"*International Energy Outlook 2016*,"In: *US Energy Information Administration,* vol. 0484,

[3] D. Yang, Y. Sheng, and M. Green, (2014)"*UCG: Where in the world*,"In: *The Chemical Engineer (872),* vol. 38-41.ISSN 0302-0797.,

[4] D. Yang, N. Koukouzas, M. Green, and Y. Sheng, (2015)"*Recent Development on Underground Coal Gasification and Subsequent CO2 Storage*,"In: *Journal of the energy institute,* vol. 89(4), pp. 469-484,

[5] K. Stańczyk, K. Kapusta, M. Wiatowski, J. Świądrowski, A. Smoliński, J. Rogut*, et al.*, (2012)"*Experimental simulation of hard coal underground gasification for hydrogen production*,"In: *Fuel,* vol. 91, pp. 40-50,

[6] L. Yang, (2003)"*Clean coal technology—Study on the pilot project experiment of underground coal gasification*,"In: *Energy,* vol. 28, pp. 1445-1460,

[7] R. Wu, (1988)"*Coal gasification*,"In: *Xuzhou: China University of Mining and Technology Press,* vol. p. 68e73.,

[8] H. Wang, B. Dlugogorski, and E. Kennedy, (2003)"*Coal oxidation at low temperatures: oxygen consumption, oxidation products, reaction mechanism and kinetic modelling*,"In: *Progress in Energy and Combustion Science,* vol. 29(6):487e513.,

[9] S. D. Yang LH, (2001)"*Study on the method of seepage combustion in underground coal gasification*,"In: *Xuzhou, China: China University of Mining and Technology Press,* pp. 61-3,

[10] CouchG, (2009)"*Underground coal gasification. London, United Kingdom*,"In: *IEA Clean Coal Centre, Report, Contract No.:CCC/151,*

[11] M. J. Shannon, C. B. Thorsness, and R. W. Hill, (1980)"*Early Cavity Growth During Forward Burn*,"In: *Report No. UCRL-84584,*

[12] Hill RW, (1981)"*Burn Cavity Growth during the Hoe Creek No. 3 Underground Coal Gasification Experiment*,"In: *Report No. UCRL-85173, US - DOE,*

[13] K. Kapusta and K. Stańczyk, (2014)"*Underground Coal Gasification in Poland : Experiences, results and future prospects*,"In: *Presentation on MINERALS ENGINEERING 2014, UK Energy Simposium,*

[14] K. Stańczyk, N. Howaniec, A. Smoliński, J. Świądrowski, K. Kapusta, M. Wiatowski*, et al.*, (2011)"*Gasification of lignite and hard coal with air and oxygen enriched air in a pilot scale ex situ reactor for underground gasification*,"In: *Fuel,* vol. 90, pp. 1953-1962,

[15] M. W. Krzysztof Kapusta, Krzysztof Stan´ czyk, (2016)"*An experimental ex-situ study of the suitability of a high moisture ortho-lignite for underground coal gasification (UCG) process*,"In:

[16] A. M. Winslow, (1976)"*Numerical Model of Coal Gasification in a Packed Bed*,"In: *Report No. UCRL-77627,*

[17] C.B. Thorsness and R. B. Rosza, (1976)"*In-Situ Coal Gasification Program: Model Calculations and Laboratory Experiments*,"In: *Report No. UCRL-78302; Lawrence Livermore National Laboratory: Livermore, CA, USA,*

[18] B. Dinsmoor, J.M. Galland, and T.F. Edgar, (1978)"*The Modeling of Cavity Formation during Underground Coal Gasification.*,"In: *J. Petroleum Technol. 1978, 30, 695–704.,*

[19] R.A. Kuyper, T.H. van der Meer, and J. Bruining, (1996)"*Simulation of Underground Gasification of Thin Coal Seams*,"In: *In Situ 1996, 20, 311–346.,*

[20] M. Khan, J. Mmbaga, A. Shirazi, J. Trivedi, Q. Liu, and R. Gupta, (2015)"*Modelling Underground Coal Gasification—A Review*,"In: *Energies,* vol. 8, pp. 12603-12668,

[21] G. Perkins and V. Sahajwalla, (2007)"*Modelling of Heat and Mass Transport Phenomena and Chemical Reaction in Underground Coal Gasification*,"In: *Chem. Eng. Res. Des. 2007, 85, 329–343.,*

[22] A. Sarraf Shirazi, S. Karimipour, and R. Gupta, (2013)"*Numerical Simulation and Evaluation of Cavity Growth in In Situ Coal Gasification*,"In: *Industrial & Engineering Chemistry Research,* vol. 52, pp. 11712-11722,
[23] A. Zogala, (2014)"*CRITICAL ANALYSIS OF UNDERGROUND COAL GASIFICATION MODELS. PART I: EQUILIBRIUM MODELS – LITERARY STUDIES*,"In: *Journal of Sustainable Mining, 13(1), 22–28.,*
[24] A. Zogala, (2014)"*Ctitical Analysis of Underground Coal Gasification Models. Part II: Kinetic and Computational Fluid Dynamics Models*,"In: *Journal of Sustainable Mining,* pp. 13(1), 29-37,
[25] A. Żogała and T. Janoszek, (2015)"*CFD simulations of influence of steam in gasification agent on parameters of UCG process*,"In: *Journal of Sustainable Mining,* vol. 14, pp. 2-11,
[26] L. Yang, (2003)"*Study on the model experiment and numerical simulation for underground coal gasification*,"In: *Fuel,* vol. 83, pp. 573-584,
[27] A. M. Salem, U. Kumar, A. N. Izaharuddin, H. Dhami, T. Sutardi, and M. C. Paul, (2017)"*Advanced Numerical Methods for the Assessment of Integrated Gasification and CHP Generation Technologies*,"In: *Coal and Bimass Gasification, Recent Advances and Future Challenges, De. Santanu et.al (editor), Springer, ISBN: 978-981-10-7334-2,* pp. 307-330.,
[28] M. L. d. Sauza-Santos, (2004)"*Solid Fuels Combustion and Gasification*,"In: *Texbook and Reference Books, . ISSN 0-8247-0971-3,*
[29] A. W. Bhutto, A. A. Bazmi, and G. Zahedi, (2013)"*Underground coal gasification: From fundamentals to applications*,"In: *Progress in Energy and Combustion Science,* vol. 39, pp. 189-214,
[30] M. M. BAUM, (1971)"*Predicting the Combustion Behaviour of Coal Particles*,"In: *Combustion Science and Technology,* vol. 3, pp. 231-243,
[31] D. J. Smoot and P. J. Smith, (1985)"*Coal Combustion and Gasification*,"In: *The Plenum Chemical Engineering series, New York,*
[32] STAR-CCM+, (Documentation 2018)"*Particle Reactions*,"In: *https://documentation.thesteveportal.plm.automation.siemens.com,*
[33] Y. A. Levendis, J. Kulbhushan., K. Reza, and A. F. Sarofim, (2011)"*Combustion behavior in air of single particles from three different coal ranks and from sugarcane bagasse*,"In: *Combustion and Flame,* vol. 158, pp. 452-465,
[34] O. Zikanov, (2012. ISBN :978-81-265-3497-5)"*Essential Computational Fluid Dynamics*,"In: *Texbook and Reference Books, Wiley-India Edition,*
[35] T.-H. Shih, Liou, W.W., Shabbir, A., Yang, Z. and Zhu, J., (1994)"*A New k-εε Eddy Viscosity Model for High Reynolds Number Turbulent Flows -- Model Development and Validation*,"In: *NASA TM 106721.,*
[36] R. Khatami, C. Stivers, and Y. A. Levendis, (2012)"*Ignition characteristics of single coal particles from three different ranks in O2/N2 and O2/CO2 atmospheres*,"In: *Combustion and Flame,* vol. 159, pp. 3554-3568,
[37] R. Khatami, C. Stivers, K. Joshi, Y. A. Levendis, and A. F. Sarofim, (2012)"*Combustion behavior of single particles from three different coal ranks and from sugar cane bagasse in O2/N2 and O2/CO2 atmospheres*,"In: *Combustion and Flame,* vol. 159, pp. 1253-1271,
[38] B. Alganash, M. C. Paul, and I. A. Watson, (2015)"*Numerical investigation of the heterogeneous combustion processes of solid fuels*,"In: *Fuel,* vol. 141, pp. 236-249,
[39] T. Sutardi, L. Wang, M. C. Paul, and N. Karimi, (2018)"*Numerical Simulation Approaches for Modelling a Single Coal Particle Combustion and Gasification*,"In: *Engineering Letters, 26:2, EL_26_2_09,*
[40] L. Wang, N. Karimi, and M. C. Paul, (2018)"*Gas-phase transport and entropy generation during transient combustion of a single biomass particle in varying oxygen and nitrogen atmospheres*,"In: *International Journal of Hydrogen Energy,* vol. 43(17), pp. 8506-8523,
[41] J. Tomeczek, (1992)"*Spalanie węgla [Coal combustion]*,"In: *Politechniki Ślqskiej.,*
[42] Z. Q. Li, Wei, F., & Jin, Y. , (2003)"*Numerical simulation of pulverized coal combustion and NO formation.*,"In: *Chemical Engineering Science, 58(23-24), 5161–5171. ,*

[43] E. A. Boiko, & Pachkovskii, S.V.A. , (2004)"*Kinetic Model of Thermochemical Transformation of Solid Organic Fuels.*,"In: *Russian Journal of Applied Chemistry, 77(9),* pp. 1547–1555.,
[44] A. Silaen, & Wang, T., (2009)" *Comparison of instantaneous, equilibrium, and finite-rate gasification models in an entrained-flow coal gasifier*,"In: *In Proceedings of the 26th International Pittsburgh Coal Conference (pp. 1–11),*
[45] C. J. Chen, Hung, C.I., & Chen, W.H. , (2012)"*Numerical investigation on performance of coal gasification under various injection patterns in an entrained flow gasifier.*,"In: *Applied Energy, 100, 218–228.,*
[46] A. Silaen, & Wang, T. , (2010)"*Effect of turbulence and devolatization models on coal gasification simulation in entrained-flow gasifier.*,"In: *International Journal of Heat and Mass Transfer, 53(9-10),* pp. 2074-2091.,
[47] H. Watanabe, & Otaka, M. , (2006)"*Numerical simulation of coal gasification in entrained flow coal gasifier.*,"In: *Fuel, 85(12-13),* pp. 935–943.,
[48] A. M. Mayers, (1934)"*The rate of reduction of carbon dioxide by graphite*,"In: *Am Chem Soc J,* vol. 56:70–6.,
[49] W. G. Howard JB, Fine DH. Fine., (1973)"*Kinetics of carbon monoxide oxidation in postflame gases*,"In: *Proceedings of 14th symposium (Int.) on combustion,* vol. p. 975–86.,
[50] Z. Sun, Wu, J., Wang, Y., Zhang, D. , (2009)"*A kinetic study of CO2 gasification of a Chinese coal char during combined coal gasification and CH4 reforming*,"In: *Journal of Fuel Chemistry and Technology, Vol. 37, No. 4, 2009, p. 410-415.,*

Table 1. Main gasification reactions for UCG application [25]

No	Reaction Name	Mechanism	Enthalpy of Reaction (kJ/mol)
R1	Devolatilization	Raw coal → Coal volatile + Char	
R2	Reaction of combustion	$C + O_2 \rightarrow CO_2$	-393
R3	Reaction of combustion	$C + 0.5O_2 \rightarrow CO$	-111
R4	Boudouard reaction	$C + CO_2 \rightarrow 2CO$	+172
R5	Water gas reaction	$C + H_2O \rightarrow CO + H_2$	+131
R6*	Methanation reaction	$C + 2H_2 \rightarrow CH_4$	-75
R7	Coal Volatile oxidation	Coal Volatile + $O_2 \rightarrow CO_2 + H_2O + N_2$	
R8	Reaction of combustion	$CO + 0.5O_2 \rightarrow CO_2$	-283
R9*	Water formation	$H_2 + 0.5O_2 \rightarrow H_2O$	-242
R10*	Water gas shift reaction	$CO + H_2O \rightarrow CO2 + H_2$	-41
R11*	Reforming of methane with steam	$CH_4 + H_2O \rightarrow CO + 3H_2$	+206
R12*	Partial oxidation of methane	$CH_4 + 0.5O_2 \rightarrow CO + 2H_2$	-36
R13*	Reforming of methane with CO2	$CH_4 + CO_2 \rightarrow 2CO + 2H_2$	+247

*Reactions included in the gasification model

Table 2. Chemical composition of the coal

Bituminous Coal - PSOC 1451	
Proximate Analysis as receives	
Moisture (%)	2.5
Volatile matter (%)	33.6
Fixed Carbon (%)	50.6
Ash (%)	13.3
Ultimate Analysis (on dry basis)	
Carbon (%)	71.9
Hydrogen (%)	4.9
Oxygen (%) (by diff.)	6.9
Nitrogen (%)	1.4
Sulfur (%)	1.4
Sodium (%)	0.06
Ash (%)	13.7
Heating value dry fuel (MJ/kg)	31.5

Table 3. Parameter of chemical kinetics from different studies[24]

Type of reaction	Reaction no	Kinetic parameters			Ref.
		A (unit vary)	E_a (j/kmol)	β	
Devolatilization	R1	3.12E+05	7.40E+07	0	[38]
Heterogeneous	R2	0.002	7.90E+07	0	[38]
		322	9.01E+07	0	[41]
		1225	9.98E+07	0	[42]
		11000	1.13E+08	0	[43]
Heterogeneous	R3	0.052	1.33E+08	0	[38, 44]
		0.002	7.90E+07	0	[45]
		3.3	6.11E+07	0	[46]
		85500	1.40E+08	0.84	[47]
Heterogeneous	R4	4.4	1.62E+08	1	[38, 46]
		0.0732	1.13E+08	0	[44]
		6.94E+04	1.85E+08	1	[41]
		242	2.75E+08	0	[45]
		7.38E+03	1.38E+08	0	[42]
		8.55E+04	1.40E+08	0.84	[47]
		7.90E+05	2.14E+08	0	[43]
Heterogeneous	R5	1.33	1.47E+08	1	[38, 46, 48]
		7.82E-02	1.15E+08	0	[44]
		4.26E+02	3.16E+08	0	[45]
		1.60E+04	1.81E+08	0	[43]
		5.96E+04	2.08E+08	0	[41]
		8.55E+04	1.40E+08	0.84	[47]
Heterogeneous	R6*	1000	1.13E+08	0	[43]
Coal volatile oxidation	R7	2.12E+11	2.03E+08	0	[38]
Homogenous	R8	1.30E+11	1.26E+08	0	[38, 49]
		2.20E+20	1.67E+07	0	[45]
		2.20E+12	1.67E+08	0	[46, 47]
		1.10E+10	1.33E+08	-0.75	[41]
Homogenous	R9*	1.50E+13	2.85E+07	0	[41]
		5.00E+10	1.68E+08	0	[45]
		6.80E+15	1.68E+08	0	[47]
Homogenous	R10*	4.20E+07	1.38E+08	0	[43]
		2.75E+02	8.38E+07	0	[46]
		2.75E+10	8.38E+07	0	[47]
Homogenous	R11*	4.40E+11	1.68E+08	0	[47]
		4.40E+03	1.68E+08	0	[45]
Homogenous	R12*	3.00E+08	1.26E+08	-1	[47]
		4.00E+03	1.26E+06	-1	[45]
Homogenous	R13*	4.60E+11	3.12E+08	0.3	[50]

Table 4. Variation of kinetic parameters value of R2 and R3

Reference value used for R2	Reference value used for R3	ID of combination
Blaid, et al. 2015,[38]	Blaid Alganash et al [38], Silaen & Wang, 2009 [44]	Simulation 1
	Silaen & Wang, 2010 [46]	Simulation 2
	Watanabe & Otaka, 2006 [47]	Simulation 3
Tomeczek, 1992 [41]	Chen Et al, 2012 [45]	Simulation 4
	Silaen & Wang, 2009 [44]	Simulation 5
	Silaen & Wang, 2010 [46]	Simulation 6
	Watanabe & Otaka, 2006 [47]	Simulation 7
Li et al, 2003 [42]	Chen Et al, 2012 [45]	Simulation 8
	Silaen & Wang, 2009 [44]	Simulation 9
	Silaen & Wang, 2010 [46]	Simulation 10
	Watanabe & Otaka, 2006 [47]	Simulation 11
Boiko & Pachkovskii, 2004 [43]	Chen Et al, 2012 [45]	Simulation 12
	Silaen & Wang, 2009 [44]	Simulation 13
	Silaen & Wang, 2010 [46]	Simulation 14
	Watanabe & Otaka, 2006 [47]	Simulation 15

Table 5. The ID for combination of Simulation 3 with R4, R5 and R8

Combination		Kinetic parameters			Ref	ID
		A (unit vary)	E_a (j/kmol)	β		
Simulation 3	R4	0.0732	1.13E+08	0	[44]	Simulation 3A-R4
		6.94E+04	1.85E+08	1	[41]	Simulation 3B-R4
		242	2.75E+08	0	[45]	Simulation 3C-R4
		7.38E+03	1.38E+08	0	[42]	Simulation 3D-R4
		8.55E+04	1.40E+08	0.84	[47]	Simulation 3E-R4
		7.90E+05	2.14E+08	0	[43]	Simulation 3F-R4
Simulation 3	R5	7.82E-02	1.15E+08	0	[44]	Simulation 3A-R5
		4.26E+02	3.16E+08	0	[45]	Simulation 3B-R5
		1.60E+04	1.81E+08	0	[43]	Simulation 3C-R5
		5.96E+04	2.08E+08	0	[41]	Simulation 3D-R5
		8.55E+04	1.40E+08	0.84	[47]	Simulation 3E-R5
Simulation 3	R8	2.20E+20	1.67E+07	0	[45]	Simulation 3A-R8
		2.20E+12	1.67E+08	0	[46] [47]	Simulation 3B-R8
		1.10E+10	1.33E+08	-0.75	[41]	Simulation 3C-R8

Table 6. Scheme for identification of kinetic parameters of gasification

Type of reaction	Reaction no	Kinetic parameters			Ref	ID
		A (unit vary)	E_a (j/kmol)	β		
Combustion/Oxidation/Simulation 3	R6	1000	1.13E+08	0	[43]	
	R9	1.50E+13	2.85E+07	0	[41]	GA-R9
		5.00E+10	1.68E+08	0	[45]	GB-R9
		6.80E+15	1.68E+08	0	[47]	GC-R9
	R10	4.20E+07	1.38E+08	0	[43]	GA-R10
		2.75E+02	8.38E+07	0	[46]	GB-R10
		2.75E+10	8.38E+07	0	[47]	GC-R10
	R11	4.40E+11	1.68E+08	0	[47]	GA-R11
		4.40E+03	1.68E+08	0	[45]	GB-R11
	R12	3.00E+08	1.26E+08	-1	[47]	GA-R12
		4.00E+03	1.26E+06	-1	[45]	GB-R12
	R13	4.60E+11	3.12E+08	0.3	[50]	

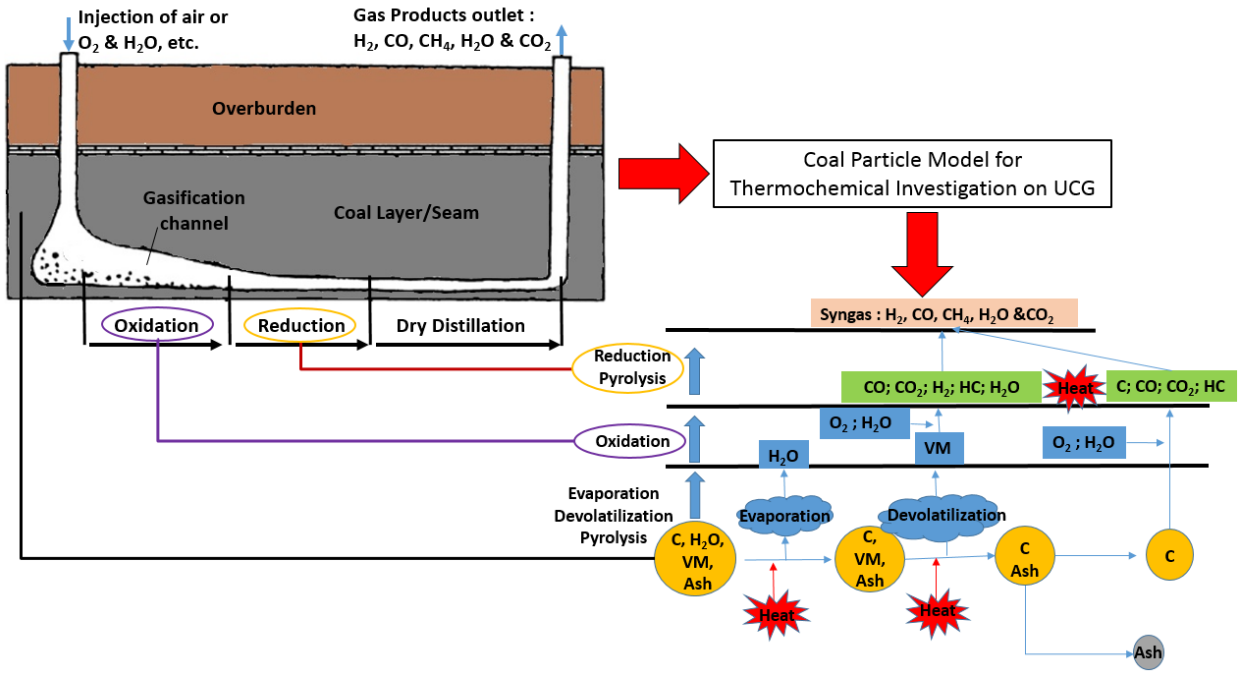

Figure 1. Process illustration of coal particle gasification model and UCG

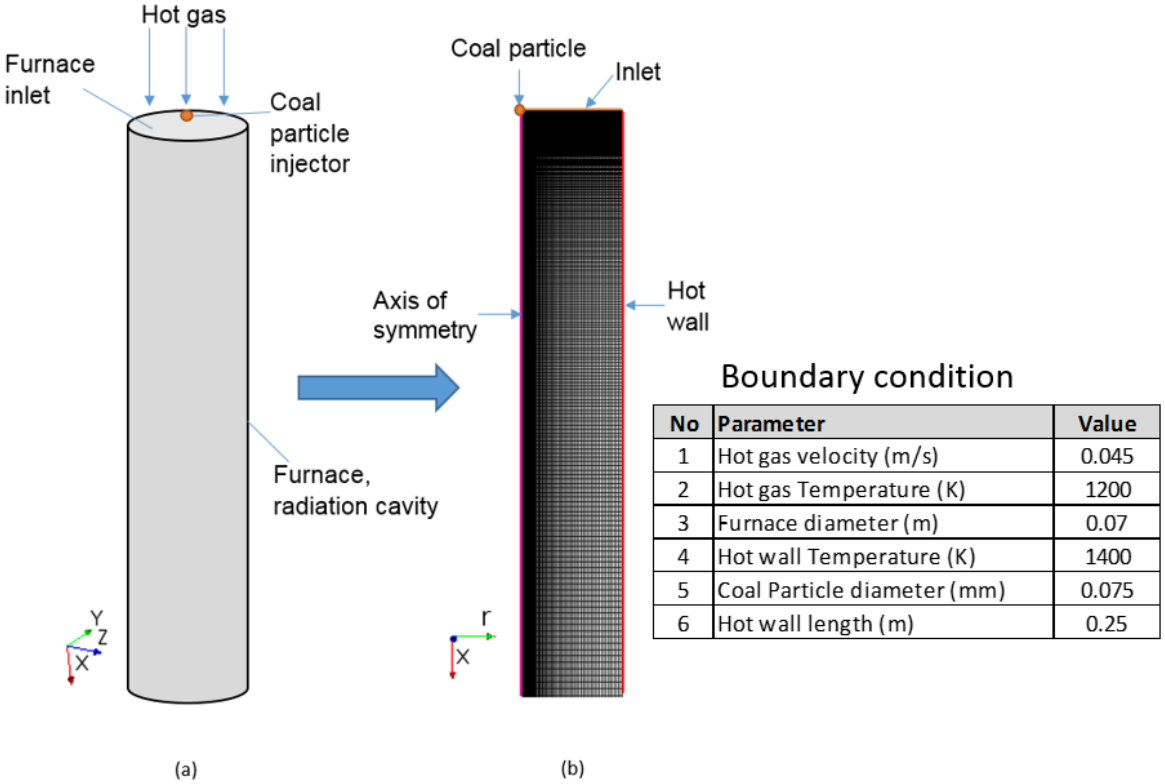

Boundary condition

No	Parameter	Value
1	Hot gas velocity (m/s)	0.045
2	Hot gas Temperature (K)	1200
3	Furnace diameter (m)	0.07
4	Hot wall Temperature (K)	1400
5	Coal Particle diameter (mm)	0.075
6	Hot wall length (m)	0.25

Figure 2. The furnace illustration (a) Furnace cylindrical shape (b) Axis symmetry model grid

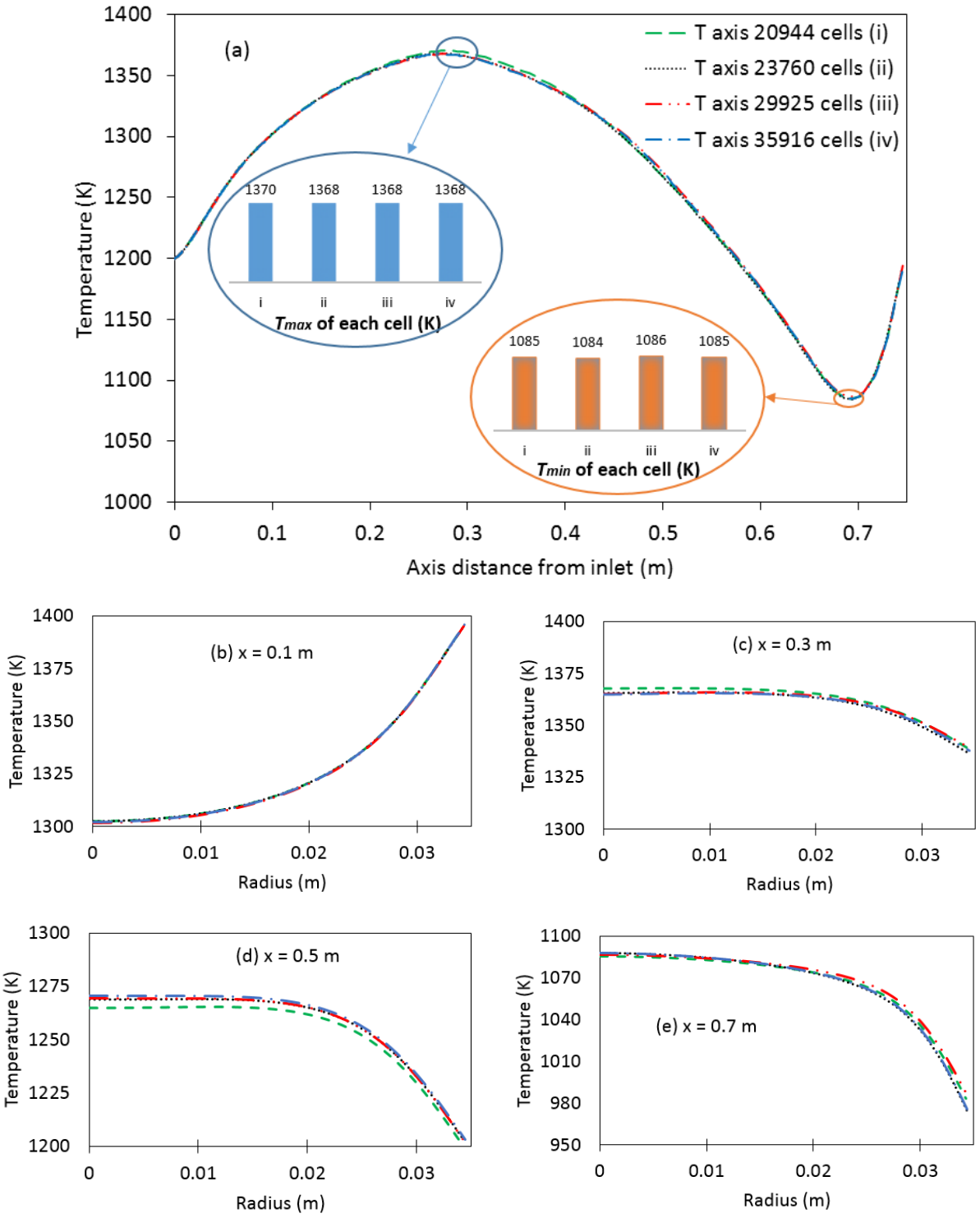

Figure 3. Grid size variation test for gas temperature (a) along the axis/center line; radial direction at (b) x = 0.1 m, (c) x = 0.3 m, (d) x = 0.5 m, and (e) x = 0.7 m

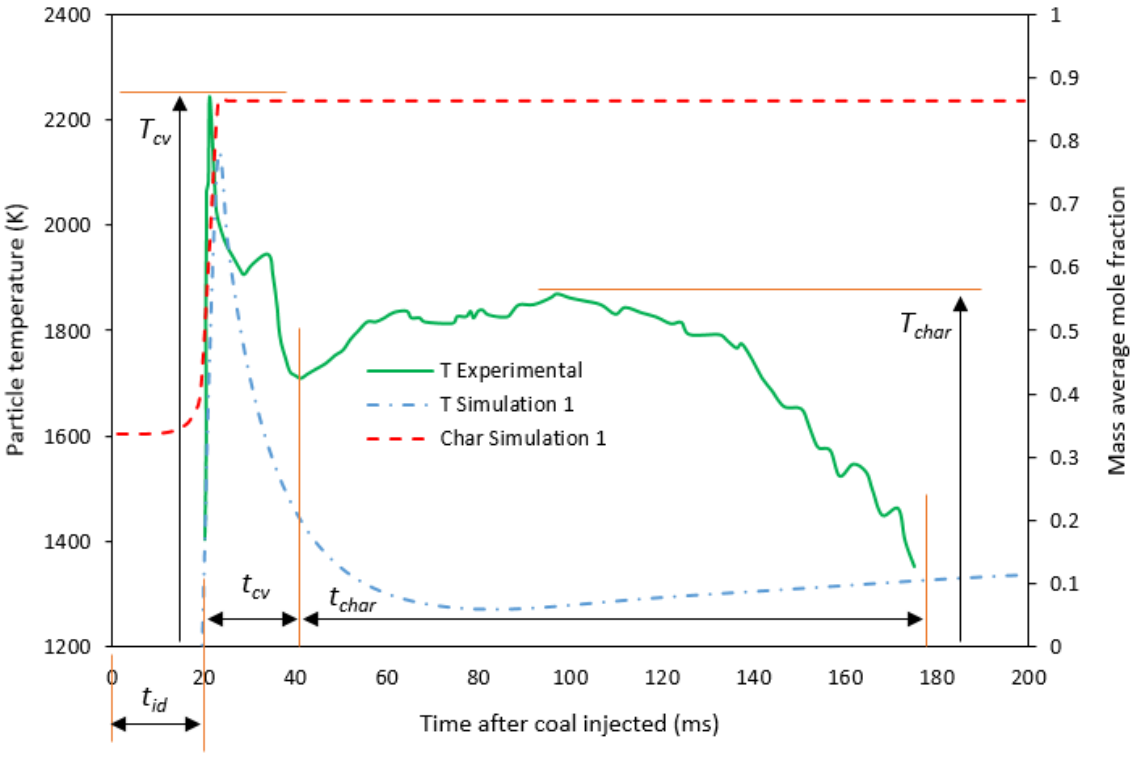

Figure 4. The comparison of Simulation 1 and experimental results

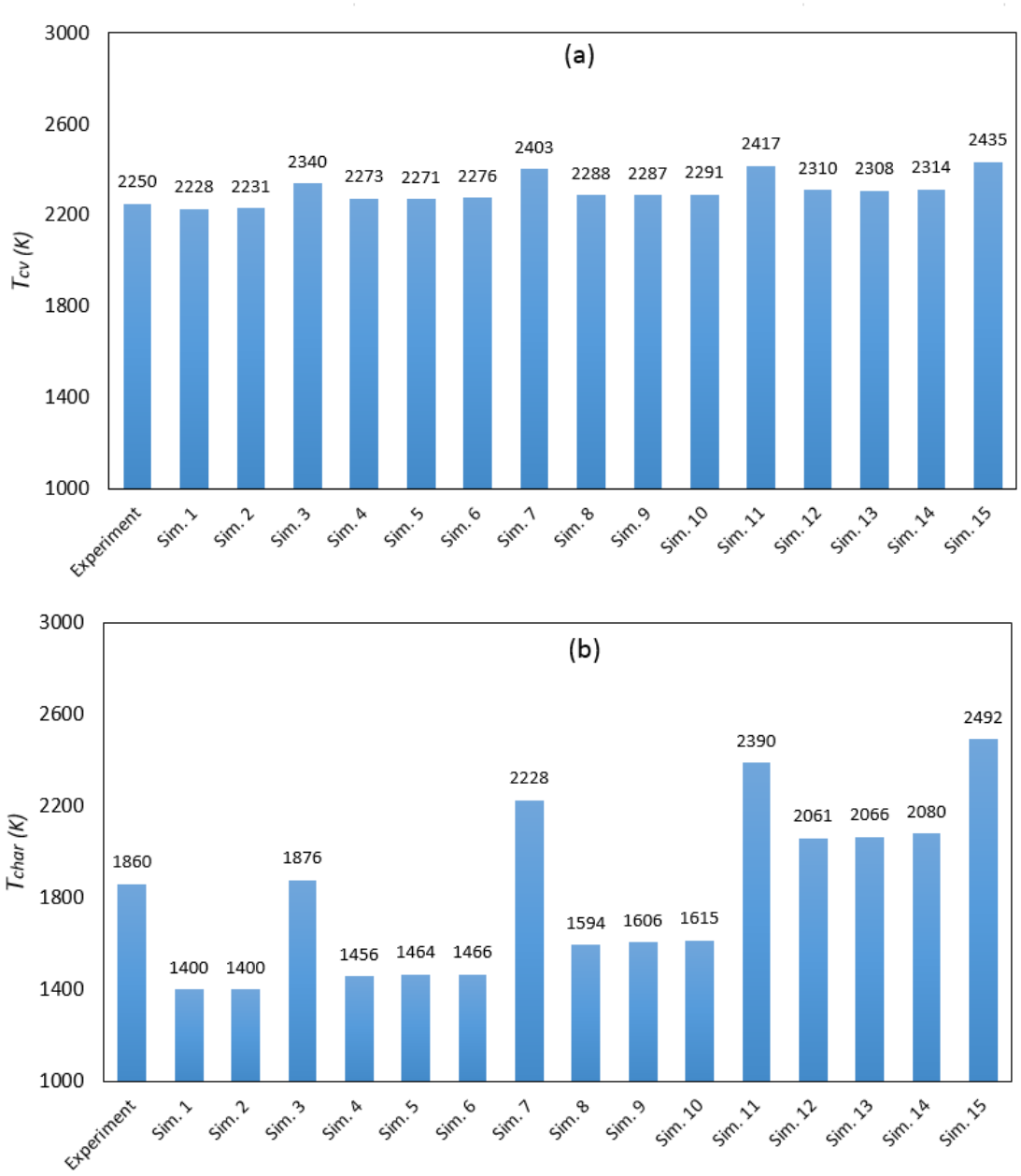

Figure 5. Comparison of simulation result for (a) T_{cv} and (b) T_{char}

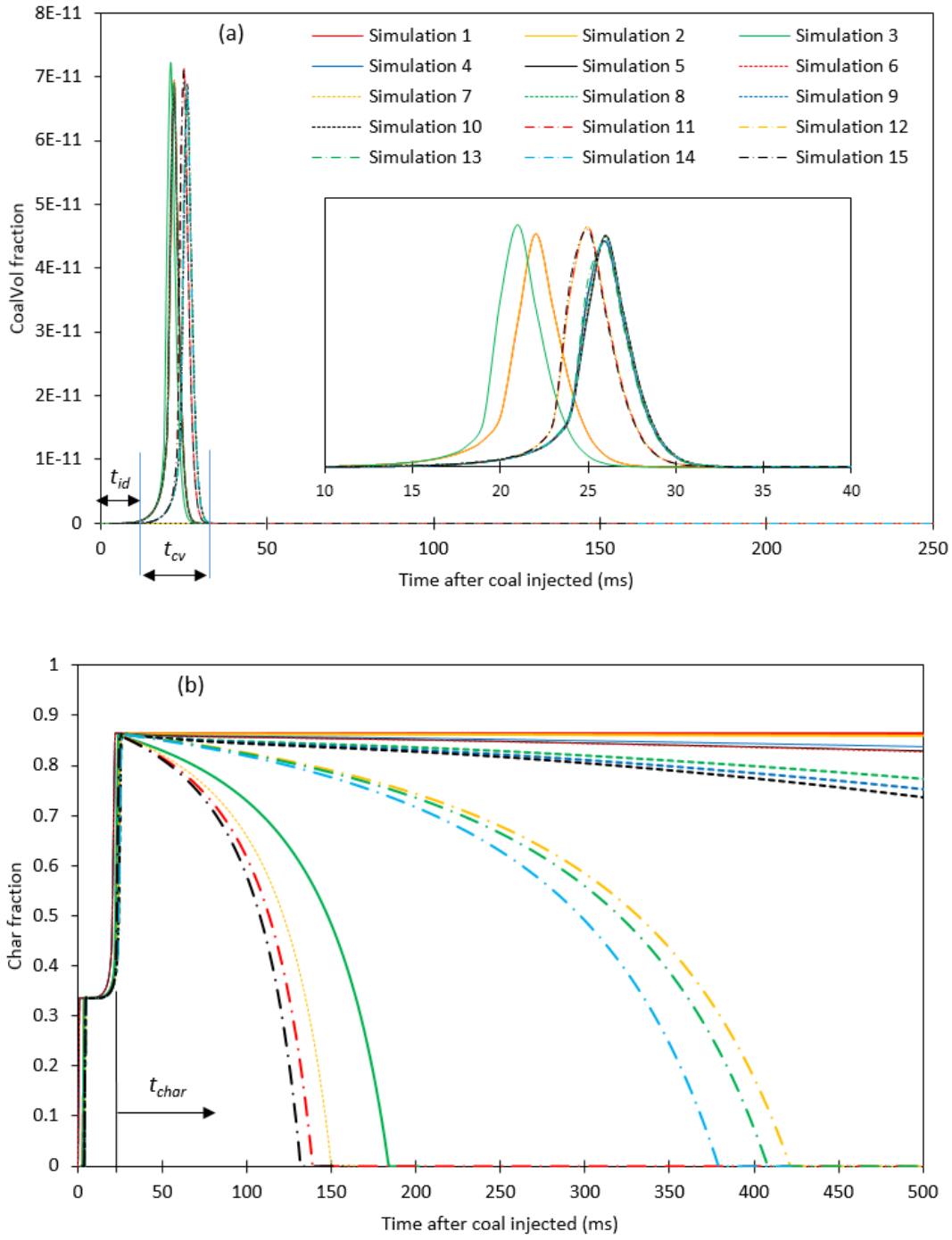

Figure 6. Comparison simulation results for (a) Coal Volatile, and (b) Char

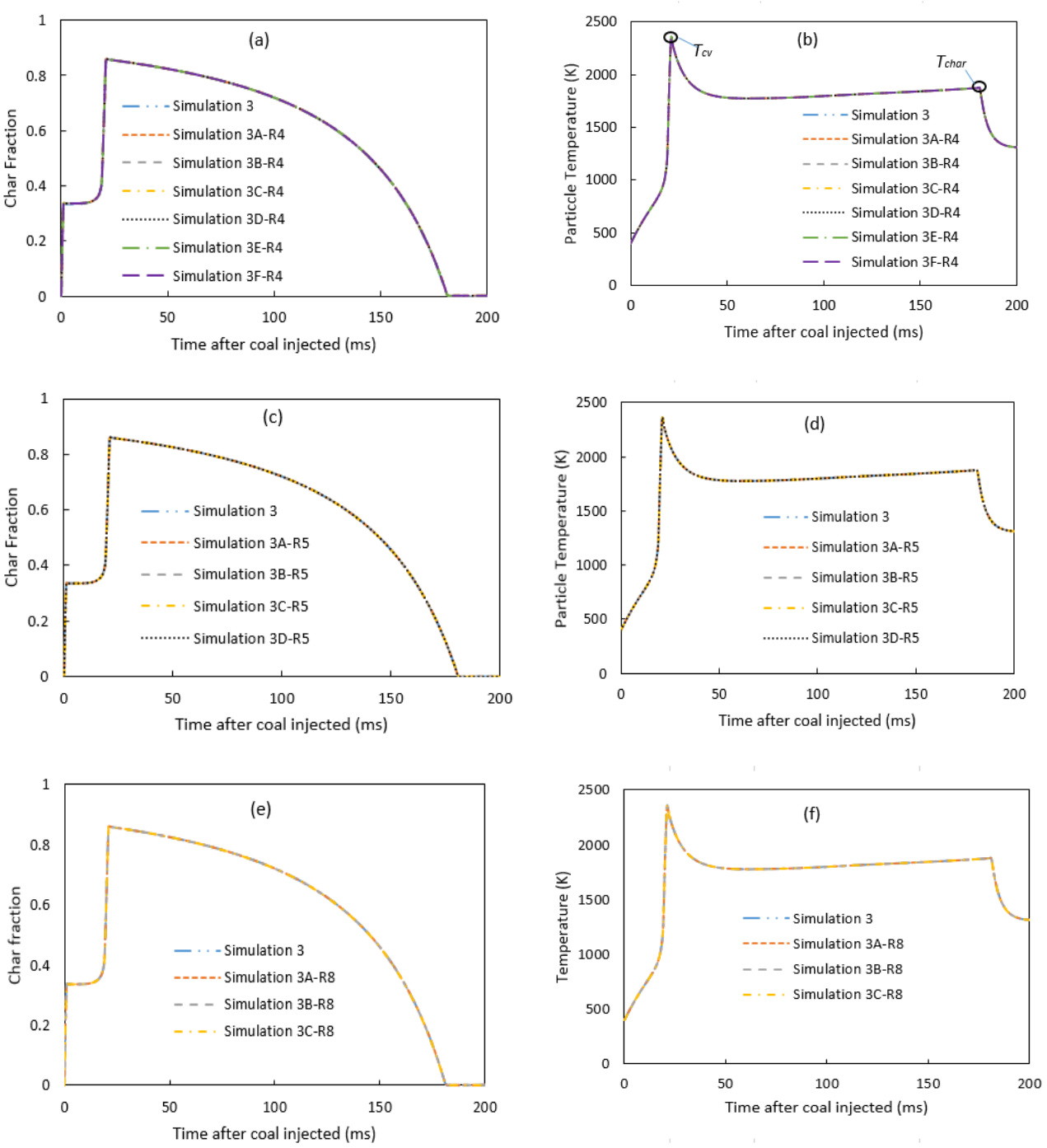

Figure 7. Variation of kinetic parameters of R4 on the (a) char fraction (b) particle temperature

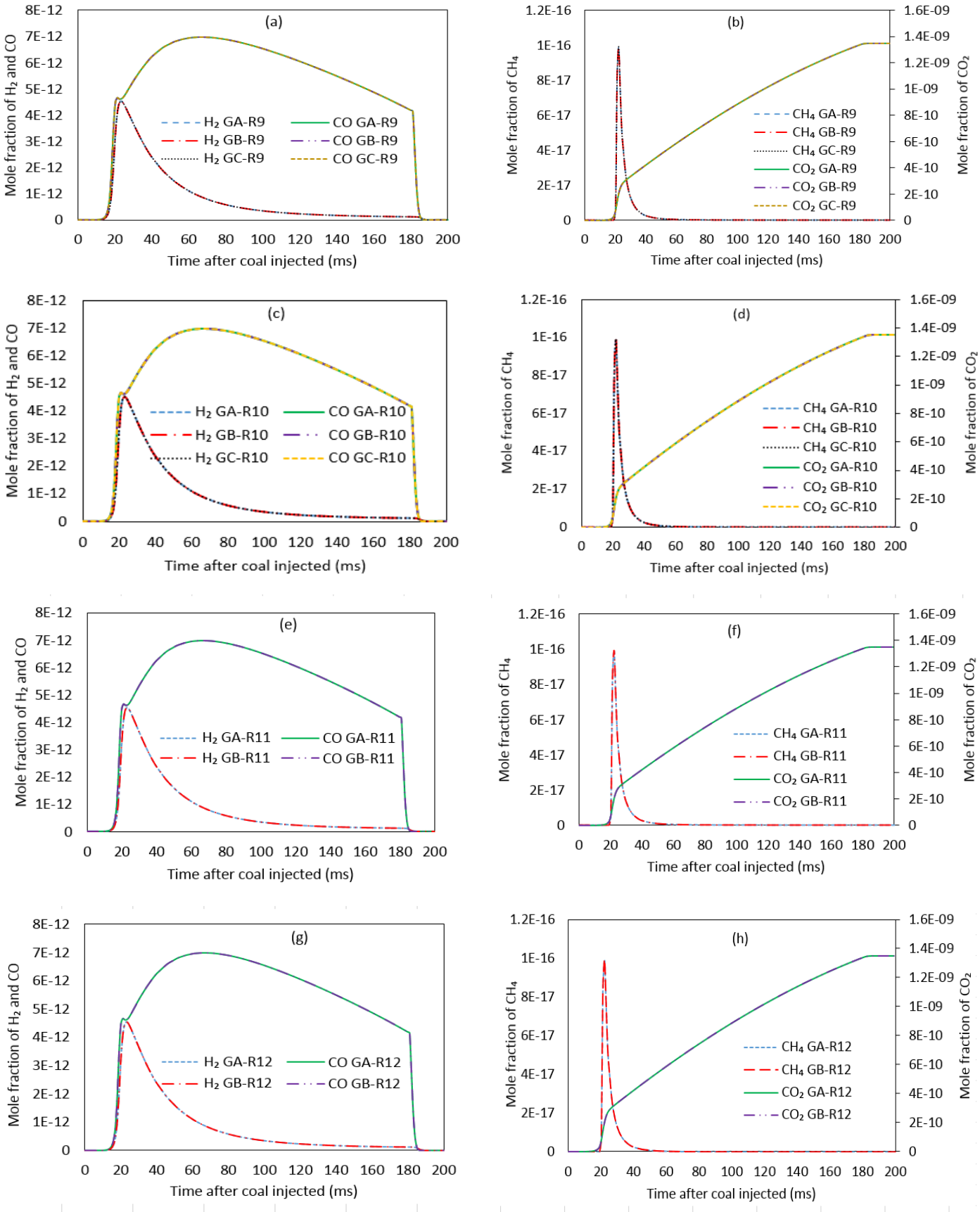

Figure 8. Comparison of gas production for reaction (a) R9* and (b) R10*

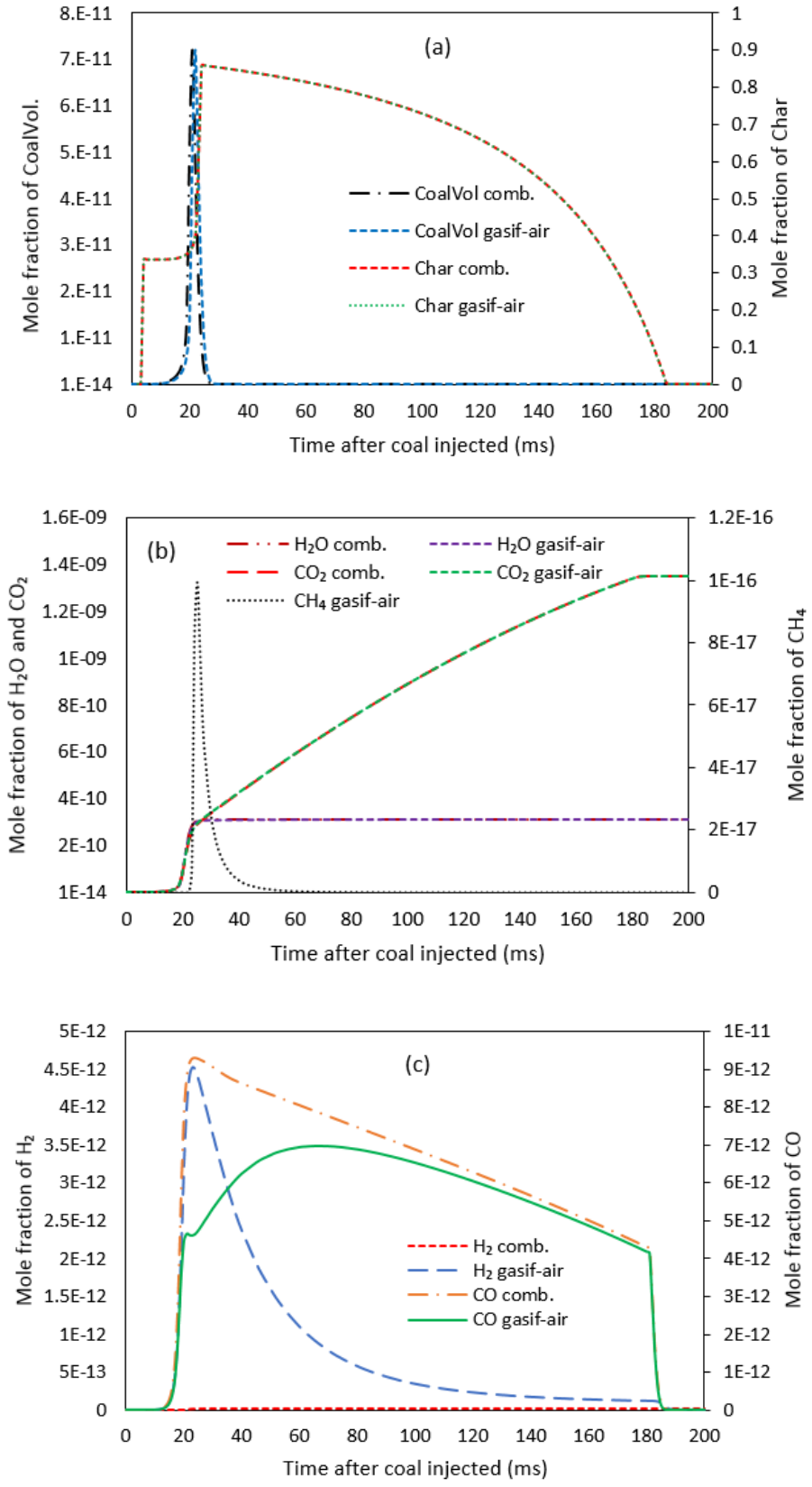

Figure 9. Comparison of the (a) CO_2, H_2O and coal volatile and (c) H_2 and CO gas species

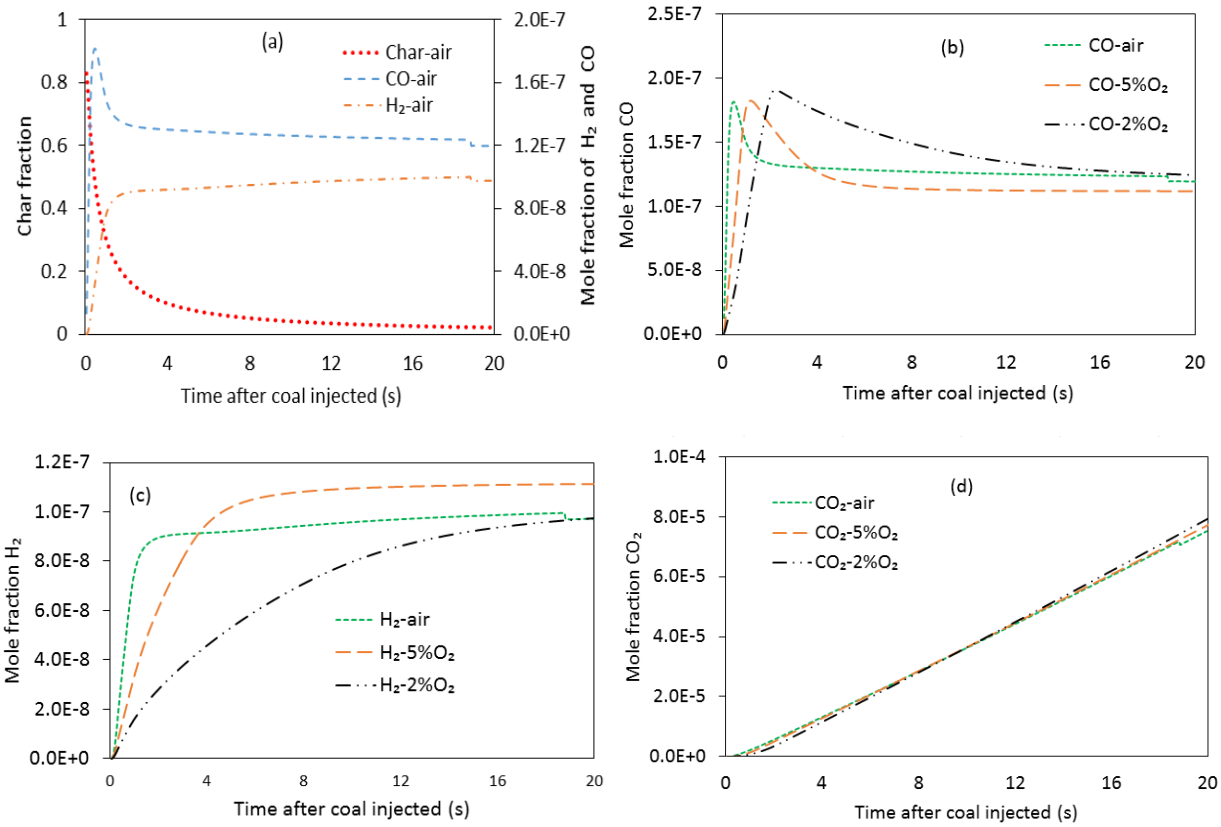

Figure 10. Simulation results of continuous injection (a) Char, CO and H_2 correlation, (b) CO products in various O_2 (c) H_2 products in various O_2, and (d) the CO_2 products in various O_2

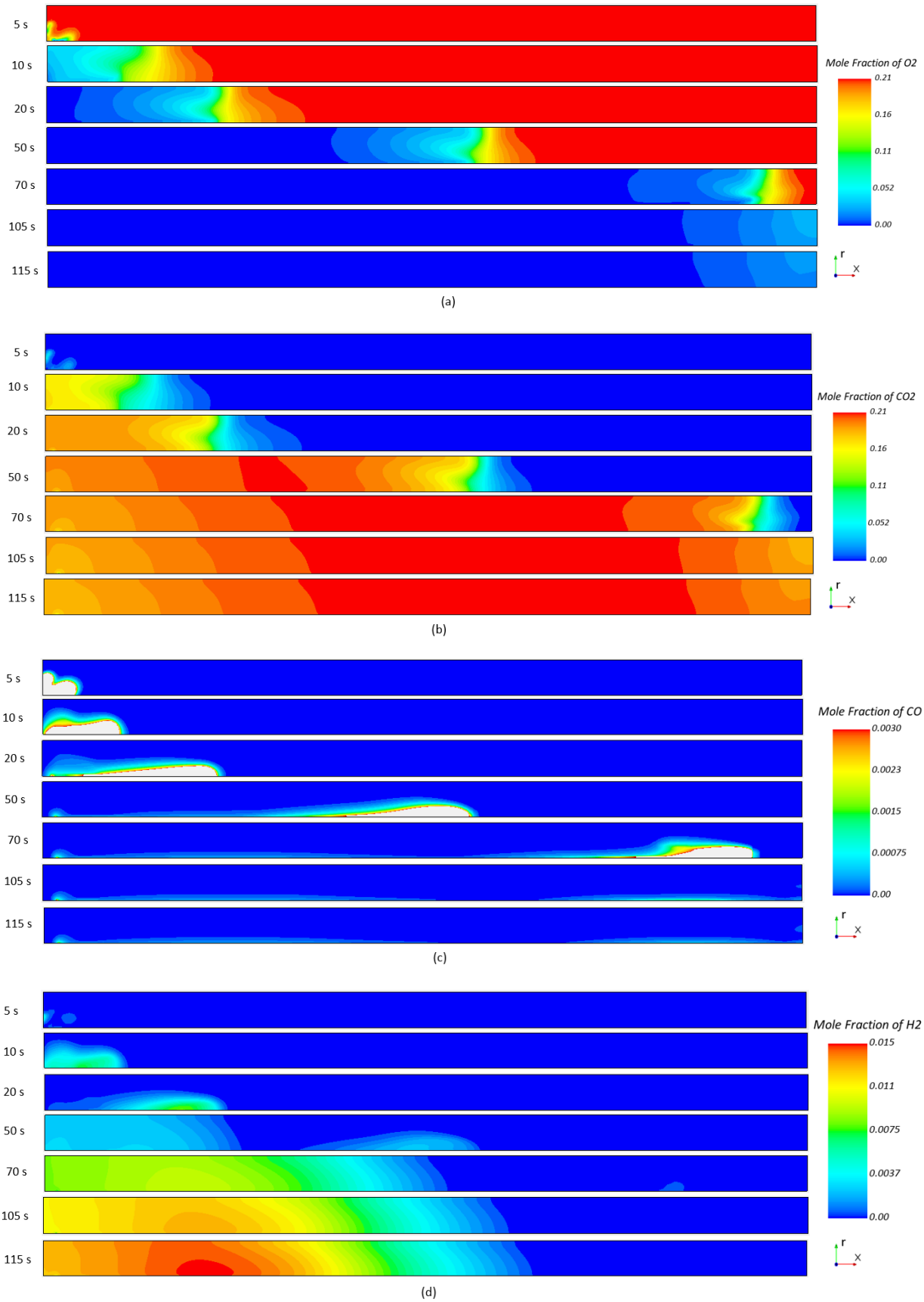

Figure 11. Contour plot of gas formation in the reactor, for (a) CO_2; (b) CO; and (c) H_2